CONTENTS

Participants

      1,601 participants completed multimodal neuroimaging as part of the PNC (1, 2), a large-scale community-based study of brain development. Of these, 154 were excluded for: medical disorders that could impact brain functioning (n=81), medication use for medical conditions that could affect central nervous system functioning (n=64), or substantial structural brain abnormalities (n=20); several subjects were excluded for multiple criteria. Exclusion criteria based on medical history included but was not limited to: cancer, cerebral meningitis, cystic fibrosis, immunological conditions (e.g., lupus, common variable immunodeficiency), lead poisoning, severe liver or kidney problems, and sickle cell anemia. Neurological/endocrine disorders that were the basis of exclusion included: epilepsy, stroke, loss of consciousness for more than 5 min, major neurodevelopmental disorders (e.g., autism), brain tumor or injury, reflex neurovascular dystrophy, Marfan syndrome, thyroid problems, and Turner syndrome. Medications for medical conditions that were the basis of exclusion included but were not limited to: anticonvulsants, antiemetics, CNS stimulants, muscle relaxants, narcotic analgesics (pain relievers), and sedatives. In addition, 51 individuals were excluded for failing to meet structural image quality assurance protocols, and two participants were excluded for missing clinical data. The final sample consisted of 1,394 youth; demographics of the sample are summarized in Table 1.

Clinical Assessment

      As described in detail in our previous work (1–3), assessment of lifetime psychopathology was conducted using GOASSESS, a structured screening interview administered to probands (age 11-21) and collateral informants of probands (age 8-17), based on a modified version of the Kiddie-Schedule for Affective Disorders and Schizophrenia (4) and Diagnostic and Statistical Manual of Mental Disorders, 4th edition, Text Revision criteria (5). The GOASSESS interview assesses lifetime occurrence of mood (major depressive episode, mania), anxiety (agoraphobia, generalized anxiety, panic, specific phobia, social phobia, separation anxiety, posttraumatic stress), behavioral problems (oppositional defiant, attention deficit/hyperactivity, conduct), psychosis, eating disorder (anorexia, bulimia), and suicidal symptoms. Among the GOASSESS questions, 112 screening items administered to all participants were used for the current investigation. Of note, due to comorbidity, participants may be represented in more than one category. The GOASSESS interview was administered by trained assessors who underwent a common training protocol (developed and implemented by Dr. Calkins) that included didactic sessions, assigned readings, and supervised pair-wise practice. Assessors were certified for independent assessments following observation by a certified clinical observer who rated the proficiency of the assessor on a 60-item checklist of interview procedures. The median interval of time between clinical assessment and neuroimaging was 2 months.

Factor Analysis

      Traditional diagnostic categories are limited by inadequate reliability, as well as substantial heterogeneity and comorbidity found among disorders (6–10). Additionally, given that psychopathology symptoms are continuous and hierarchically arranged (11–13), we sought to quantify a dimensional measure of psychopathology across all psychiatric disorders. To do this, we applied an exploratory factor analysis (EFA) to 112 item-level symptom questions from the GOASSESS. EFA is used to find meaningful patterns of covariance and to optimally cluster variables by identifying a smaller number of unobserved variables, or factors, that explain said

covariance. For example, it is possible that covariances among our 112 symptom variables mainly reflect the influence of a smaller number of underlying (latent) variables. Exploratory factor analysis aims to identify these latent variables in an exploratory manner, in other words, without imposing any constraints based on *a priori* theories about how the variables will be related. As described in detail elsewhere (14), an exploratory factor analysis with the PNC dataset yielded four correlated dimensions of psychopathology including factors for anxious-misery, psychosis, behavioral (externalizing), and fear (Figure 1A). This is consistent with the results of prior exploratory factor analyses of psychiatric symptoms (11, 12, 15). Importantly, these factors are highly correlated with one another and lack specificity. For example, as can be seen in Figure 1A, the participants with fear-based disorders (PTSD, agoraphobia, social anxiety, specific phobia, and separation anxiety) had the highest scores on the fear factor, but also had fairly high scores on the three other factors (anxious-misery, psychosis, and behavioral) as well. Additionally, we see that the fear factor is fairly high across all of the symptom categories (e.g., depression, GAD, psychosis, ADHD, conduct disorder, etc.). Thus, endorsement of any of the 112 psychiatric symptoms increases the probability of endorsement of any other of the symptoms, regardless of whether the symptoms are part of the same disorder. This implies that there may be a "general" latent variable explaining at least some of the covariance across all psychiatric symptoms. However, exploratory factor analysis with a simple-structure oblique (oblimin) rotation does not capture this common factor.

The common factor among psychopathology disorders has been termed "*p*" for psychopathology, akin to the overall "*g*" intelligence factor in cognition research (13). Like *g*, the *p* factor quantifies the overall level of psychopathology present across clinical domains. Importantly, *p* has been identified as an important feature of clinical symptoms that may contribute to the non-specificity of biomarkers found across disorders (10); thus, the *p* factor was of direct interest to the current study. To measure the *p* factor, we use a bifactor model, which requires each item to load on a primary dimension of interest and no more than one secondary dimension. In other words, the bifactor model identifies a common factor that is shared across all 112 symptoms while simultaneously estimating specific symptom factors (e.g., anxious-misery, psychosis, behavioral, and fear); the general factor ("*p*") and the group factors compete for explanation of variance in the item (symptom) responses. Thus, the bifactor model yields both the *p* factor and orthogonal (uncorrelated) factors for the specific dimensions of symptoms. As documented in full elsewhere (14), we used a confirmatory bifactor analysis (16, 17) implemented in Mplus (18) to model the four correlated factors found with exploratory factor analysis (anxious-misery, psychosis, behavioral, and fear) plus a fifth factor that was common across all psychiatric disorders, which we termed overall psychopathology (Figure 1B). The scores for each factor from the bifactor model showed excellent reliability (overall psychopathology: alpha = .98, anxious-misery: alpha = .82, psychosis: alpha = .80, behavioral: alpha = .92, fear: alpha = .85). Note that by including the general factor for overall psychopathology, correlations among the four specific factors were removed—i.e. all factors in the bifactor model are orthogonal. The use of a bifactor model is critical for increasing the specificity of our factors. For example, Figure 1C demonstrates how the orthogonal factors now relate more specifically to the relevant disorders using the bifactor model, relative to the exploratory factor analysis model (Figure 1A). Additionally, as can be seen in Figure 1C, overall psychopathology in the green bars was common across the diagnostic categories, but had the strongest associations with the psychosis and anxious-misery disorders followed by the behavioral and fear disorders. By extracting overall psychopathology (*p* factor) from the model,

the anxious-misery, psychosis, behavioral, and fear factors now represent the "pure" symptoms not accounted for by general psychopathology. For example, the fear factor represents the fear symptoms specific to the fear disorders and that are not shared across other diagnostic categories.

Examples of some of the items with high loadings (above .60) on the overall psychopathology factor included: 1) Has there ever been a time when you felt so full of energy that you couldn't stop doing things and didn't get tired; 2) Have you ever been bothered by thoughts that don't make sense to you, that come over and over again and won't go away, such as fear that you would do something/say something bad without intending to; 3) I have had the experience of hearing faint or clear sounds of people or a person mumbling or talking when there is no one near me; 4) Has there ever been a time when you felt grouchy, irritable or in a bad mood most of the time, even little things would make you mad; 5) Has there ever been a time when all of a sudden, you felt that you were losing control, something terrible was going to happen, that you were going crazy, or going to die? Examples of the top items for anxious-misery included: 1) Did you worry a lot more than most children/people your age; 2) Have you ever been a worrier; 3) Has there ever been a time when you felt sad or depressed most of the time; 4) Has there ever been a time when you cried a lot, or felt like crying? For psychosis, top items included: 1) I think I might feel like my mind is "playing tricks" on me; 2) I may have felt that there could possibly be something interrupting or controlling my thoughts, feelings, or actions; 3) I think I may get confused at times whether something I experience or perceive may be real or may be just part of my imagination or dreams; 4) I believe that I have special natural or supernatural gifts beyond my talents and natural strengths. For behavioral, the top items were: 1) Did you often have problems following instructions and often fail to finish school, work, or other things you meant to get done; 2) Did you often have trouble paying attention or keeping your mind on your school, work, chores, or other activities that you were doing; 3) Did you often have people tell you that you did not seem to be listening when they spoke to you or that you were daydreaming; 4) Did you often dislike, avoid, or put off school or homework (or any other activity requiring concentration)? And finally, for fear the top items included: 1) Was there ever a time in your life when you felt afraid or uncomfortable acting, performing, giving a talk/speech, playing a sport or doing a musical performance, or taking an important test or exam (even though you studied enough); 2) Felt afraid or uncomfortable when you had to do something in front of a group of people, like speaking in class; 3) Felt afraid or uncomfortable because you were the center of attention and were concerned something embarrassing might happen; 4) Felt afraid or uncomfortable or really, really shy with people, like meeting new people, going to parties, or eating or drinking, writing or doing homework in front of others? For the loadings (standardized item-trait correlations) for all items in these models, see Moore et al. (14).

Cognitive Assessment

Cognition was assessed using the University of Pennsylvania Computerized Neurocognitive Battery (CNB), which has been described in detail elsewhere (19). Briefly, 14 cognitive tests evaluating aspects of cognition, including executive control, episodic memory, complex reasoning, social cognition, and sensorimotor speed were administered in a fixed order. Except for the sensorimotor tests that only measure speed, each test provides measures of both accuracy and speed. We used three factor scores for performance accuracy derived in a previously reported exploratory factor analysis with oblique rotation (19): 1) executive function and complex reasoning, 2) social cognition, and 3) episodic memory. These cognitive factor scores were included as predictors of psychopathology in the multivariate analyses.

Image Acquisition and Processing

Imaging data were acquired on a Siemens TIM Trio 3 Tesla scanner (Erlangen, Germany) with a 32-channel head coil. Structural brain imaging was completed using a magnetization-prepared, rapid acquisition gradient-echo (MPRAGE) T1-weighted image with the following parameters: TR 1810 ms; TE 3.51 ms; FOV 180x240 mm; matrix 192x256; 160 slices; slice thickness/gap 1/0 mm; TI 1100 ms; flip angle 9 degrees; effective voxel resolution of 0.93 x 0.93 x 1.00 mm; total acquisition time 3:28 minutes. Structural image processing utilized Advanced Normalization Tools (ANTs) (20). This pipeline includes N4 bias field correction, brain extraction, Atropos probabilistic tissue segmentation (21), and direct estimation of cortical thickness in volumetric space (22). Structural images were registered to a custom adolescent template in local space using the top-performing SyN diffeomorphic registration method (23). Prior to analysis, cortical thickness images were down-sampled to 2 mm voxels and smoothed with a 4 mm full-width, half maximum Gaussian kernel. After statistical testing, images were registered to the Montreal Neurologic Institute (MNI) 152 1-mm template space for reporting of standard coordinates and display.

Image Quality Assurance

Three highly trained image analysts independently assessed structural image quality; for full details of this procedure see Rosen et al. (24). Briefly, three raters were trained prior to rating images on an independent training sample of 100 images. All three raters were trained to >85% concordance with faculty consensus ratings. T1 images were rated on a 0-2 Likert scale (0 = unusable images (3.1% of the sample), 1 = usable images with some artifact (16.9%), and 2 = images with none or almost no artifact (80.0%)). All images with an average rating of 0 were excluded from analyses. We included average quality rating across the three raters as a covariate in all models in order to control for the confounding influence of subtle variation in image quality.

All processed data underwent rigorous quality control as well. Specifically, the volume and thickness of anatomically-defined regions of interest (defined using multi-atlas labeling with joint label fusion (25); see below) were evaluated for outliers. Outliers were defined as values greater or less than 2.5 standard deviations (S.D.) from the mean regional value. Participants with an elevated (+2.5 S.D.) number of regions with outlying volume or cortical thickness values were flagged for manual review. Similarly, a regional laterality index was calculated for both cortical thickness and volume, and participants with an elevated number of regional laterality outliers (+2.5 S.D.) were flagged for review. Flagged images were then manually viewed by two independent data analysts. A total of 61 individuals were excluded for failing to meet these image processing quality assurance procedures.

Jacobian Volume

Volume images were created from the log transformed determinant of the Jacobian of the deformation field. Specifically, displacement vectors created during spatial normalization were composed with the corresponding 12-DOF affine transformation to produce total displacements from the subject brain to the template brain in millimeters. These displacement vectors were used to calculate Jacobian matrices in each voxel, on which we calculated the log of the determinant to quantify local expansion or contraction (26, 27). Our method differs from prior approaches in

that displacement vectors are usually evaluated after the affine transform has been applied, which obscures overall larger-scale changes in brain size.

Non-negative Matrix Factorization

Non-negative matrix factorization (NMF) provides several advantages over prior methods such as principal component analysis (PCA). Notably, PCA and other techniques produce widely-dispersed components with both positive and negative directions, often limiting straightforward interpretation. In contrast, NMF produces compact, positively-signed components that are more interpretable and reproducible (28, 29).

We used the same procedures for deriving networks with NMF as done previously (28, 30–32). To derive NMF networks, first the NMF algorithm takes an input matrix X containing voxel-wise cortical thickness estimates (dimensions: 128,155 voxels x 1,394 participants), and the algorithm then approximates that matrix as a product of two matrices with non-negative elements: $X \cong BC$ (Figure S1). The first matrix, B, is of size V x K and contains the estimated non-negative networks and their respective loadings on each of the V voxels, where K is the user-specified number of networks. The B matrix, or loadings matrix, is composed of coefficients that denote the relative contribution of each voxel to a given network. These non-negative coefficients of the decomposition represent the entirety of the brain as a subject-specific addition of various parts. The second matrix, C, is of size K x N and contains subject-specific weights for each network. These subject-specific weights indicate the contribution of each network in reconstructing the original cortical thickness map and were evaluated for associations with psychopathology.

Consistent with studies using this technique (28, 32), we performed multiple NMF solutions requesting 2 to 30 networks (in steps of two) in order to obtain a range of possible solutions. We selected the optimal dimensionality of these networks using two criteria. First, we calculated the reconstruction error for each solution as the Frobenius norm between the structural data matrix and the NMF approximation and plotted the reconstruction error for all solutions. Second, we conducted a split-half reliability analysis to describe the stability of the NMF solution at each resolution, quantified using the Adjusted Rand Index (ARI). As expected, reconstruction error generally declined as the number of networks increased. The final 18-network solution was chosen based on the gradient of reconstruction error (Figure S2), which shows only nominal decrements in error beyond 14 networks. Additionally, we checked the split-half reliability at this resolution, which revealed an ARI of .93 for the 18-network solution, suggesting that this solution is highly reproducible. This resolution is also consistent with previous reports (32). Accordingly, the 18-network solution was used for all subsequent analyses. As in prior work using NMF (28, 32), the structural covariance networks identified were highly symmetric bilaterally (Figure 2). Cortical thickness NMF networks were then applied to volume images in order to obtain comparable networks for volume analyses. NMF networks were visualized on the inflated Population-Average, Landmark-, and Surface-based (PALS) cortical surfaces using Caret software (33, 34). Images were converted to the Montreal Neurologic Institute (MNI) 152 1-mm template space for display.

References

1. Satterthwaite TD, Connolly JJ, Ruparel K, et al.: The Philadelphia Neurodevelopmental Cohort: A publicly available resource for the study of normal and abnormal brain development in youth. Neuroimage 2016; 124:1115–1119
2. Satterthwaite TD, Elliott MA, Ruparel K, et al.: Neuroimaging of the Philadelphia Neurodevelopmental Cohort. Neuroimage 2014; 86:544–553
3. Calkins ME, Merikangas KR, Moore TM, et al.: The Philadelphia Neurodevelopmental Cohort: constructing a deep phenotyping collaborative. J Child Psychol Psychiatry 2015; 56:1356–1369
4. Kaufman J, Birmaher B, Brent D, et al.: Schedule for Affective Disorders and Schizophrenia for School-Age Children-Present and Lifetime Version (K-SADS-PL): Initial Reliability and Validity Data. J Am Acad Child Adolesc Psychiatry 1997; 36:980–988
5. American Psychiatric Association: Diagnostic and Statistical Manual of Mental Health Disorders, Fourth Edition, Text Revision. 4th Ed., T. Washington, D.C., American Psychiatric Association, 2000
6. Galatzer-Levy IR, Bryant RA: 636,120 Ways to Have Posttraumatic Stress Disorder. Perspect Psychol Sci 2013; 8:651–662
7. Fried E: Moving forward: how depression heterogeneity hinders progress in treatment and research. Expert Rev Neurother 2017; 17:423–425
8. Regier DA, Narrow WE, Clarke DE, et al.: DSM-5 Field Trials in the United States and Canada, Part II: Test-Retest Reliability of Selected Categorical Diagnoses. Am J Psychiatry 2013; 170:59–70
9. Olbert CM, Gala GJ, Tupler LA: Quantifying heterogeneity attributable to polythetic diagnostic criteria: Theoretical framework and empirical application. J Abnorm Psychol 2014; 123:452–462
10. Shackman AJ, Fox AS: Getting Serious about Variation: Lessons for Clinical Neuroscience (A Commentary on 'The Myth of Optimality in Clinical Neuroscience'). Trends Cogn Sci 2018; 22:368–369
11. Conway CC, Forbes MK, Forbush KT, et al.: A hierarchical taxonomy of psychopathology can transform mental health research. Perspect Psychol Sci 2019; in press
12. Zald DH, Lahey BB: Implications of the Hierarchical Structure of Psychopathology for Psychiatric Neuroimaging. Biol Psychiatry Cogn Neurosci Neuroimaging 2017; 2:310–317
13. Caspi A, Moffitt TE: All for one and one for all: Mental disorders in one dimension. Am J Psychiatry 2018; 175:831–844
14. Moore TM, Calkins ME, Satterthwaite TD, et al.: Development, validation, and public release of a computerized adaptive (CAT) screener for overall mental illness burden2019; under review
15. Lahey BB, Applegate B, Hakes JK, et al.: Is There a general factor of prevalent psychopathology during adulthood? J Abnorm Psychol 2012; 121:971–977
16. Reise SP, Moore TM, Haviland MG: Bifactor models and rotations: Exploring the extent to which multidimensional data yield univocal scale scores. J Pers Assess 2010; 92:544–559

17. Gibbons RD, Hedeker DR: Full-information item bi-factor analysis. Psychometrika 1992; 57:423–436

18. Muthén L, Muthén B: Mplus The Comprehensive Modelling Program for Applied Researchers: Users Guide. Los Angeles, CA, Muthén and Muthén, 2012

19. Moore TM, Reise SP, Gur RE, et al.: Psychometric properties of the Penn Computerized Neurocognitive Battery. Neuropsychology 2015; 29:235–46

20. Tustison NJ, Cook PA, Klein A, et al.: Large-scale evaluation of ANTs and FreeSurfer cortical thickness measurements. Neuroimage 2014; 99:166–179

21. Avants BB, Tustison NJ, Wu J, et al.: An open source multivariate framework for N-tissue segmentation with evaluation on public data. Neuroinformatics 2011; 9:381–400

22. Das SR, Avants BB, Grossman M, et al.: Registration based cortical thickness measurement. Neuroimage 2009; 45:867–879

23. Avants BB, Tustison NJ, Song G, et al.: A reproducible evaluation of ANTs similarity metric performance in brain image registration. Neuroimage 2011; 54:2033–2044

24. Rosen AFG, Roalf DR, Ruparel K, et al.: Quantitative assessment of structural image quality. Neuroimage 2018; 169:407–418

25. Wang H, Suh JW, Das SR, et al.: Multi-atlas segmentation with joint label fusion. IEEE Trans Pattern Anal Mach Intell 2013; 35:611–623

26. Yanovsky I, Leow AD, Lee S, et al.: Comparing registration methods for mapping brain change using tensor-based morphometry. Med Image Anal 2009; 13:679–700

27. Yushkevich PA, Avants BB, Das SR, et al.: Bias in estimation of hippocampal atrophy using deformation-based morphometry arises from asymmetric global normalization: An illustration in ADNI 3 T MRI data. Neuroimage 2010; 50:434–445

28. Sotiras A, Resnick SM, Davatzikos C: Finding imaging patterns of structural covariance via Non-Negative Matrix Factorization. Neuroimage 2015; 108:1–16

29. Lee DD, Seung HS: Learning the parts of objects by non-negative matrix factorization. Nature 1999; 401:788–791

30. Nassar R, Kaczkurkin AN, Xia CH, et al.: Gestational age is dimensionally associated with structural brain network abnormalities across development. Cereb Cortex 2018; in press

31. Pehlivanova M, Wolf DH, Sotiras A, et al.: Diminished cortical thickness is associated with impulsive choice in adolescence. J Neurosci 2018; in press

32. Sotiras A, Toledo JB, Gur RE, et al.: Patterns of coordinated cortical remodeling during adolescence and their associations with functional specialization and evolutionary expansion. Proc Natl Acad Sci 2017; 114:3527–3532

33. Van Essen DC: A Population-Average, Landmark- and Surface-based (PALS) atlas of human cerebral cortex. Neuroimage 2005; 28:635–662

34. Van Essen DC, Drury HA, Dickson J, et al.: An integrated software suite for surface-based analyses of cerebral cortex. J Am Med Inform Assoc 2001; 8:443–59

TABLE S1. Structural covariance networks of cortical thickness in relation to anxious-misery, psychosis, behavioral, fear, and overall pathology (n=1394, df=1385)

Cortical Thickness NMF Network	Anxious-misery				Psychosis				Behavioral			
	B	SE	t	p_{fdr}	B	SE	t	p_{fdr}	B	SE	t	p_{fdr}
1: Cingulate cortex	-0.01	0.02	-0.38	.910	-0.01	0.02	-0.52	.725	-0.04	0.02	-1.77	.191
2: Medial temporal cortex	0.02	0.03	0.81	.629	-0.05	0.02	-1.99	.139	0.00	0.02	0.09	.928
3: Temporal pole	0.04	0.02	1.80	.216	-0.04	0.02	-1.82	.162	-0.03	0.02	-1.59	.222
4: Frontal cortex	-0.04	0.02	-1.84	.216	-0.02	0.02	-0.97	.500	-0.01	0.02	-0.55	.619
5: Posterior cingulate cortex	0.06	0.02	2.40	.098	-0.06	0.02	-3.04	.043	-0.04	0.02	-2.01	.191
6: Superior parietal cortex	0.02	0.02	0.81	.629	-0.02	0.02	-0.81	.537	-0.03	0.02	-1.24	.323
7: Superior temporal cortex	0.01	0.03	0.19	.931	-0.05	0.02	-2.10	.129	-0.04	0.02	-1.72	.191
8: Dorsomedial prefrontal cortex	-0.03	0.02	-1.40	.412	0.00	0.02	-0.13	.897	-0.02	0.02	-0.98	.394
9: Insular cortex	0.01	0.02	0.30	.920	-0.03	0.02	-1.44	.246	-0.04	0.02	-1.89	.191
10: Fusiform cortex	0.03	0.03	1.03	.609	-0.04	0.02	-1.47	.246	-0.05	0.03	-1.80	.191
11: Inferior temporal cortex	0.00	0.02	0.15	.931	-0.01	0.02	-0.32	.789	-0.03	0.02	-1.25	.323
12: Right lateral occipital cortex	0.05	0.03	2.03	.189	-0.04	0.02	-1.54	.246	-0.05	0.02	-1.90	.191
13: Subgenual cingulate, anterior cingulate, and anterior insula	0.01	0.02	0.53	.821	-0.04	0.02	-1.80	.162	-0.02	0.02	-0.91	.407
14: Inferior prefrontal cortex	0.00	0.02	-0.09	.931	-0.01	0.02	-0.46	.728	-0.03	0.02	-1.17	.328
15: Intraparietal	0.06	0.02	2.57	.093	-0.05	0.02	-2.12	.129	-0.05	0.02	-2.15	.191
16: Posterior cingulate (a) and TPJ (b)	0.07	0.02	2.94	.060	-0.05	0.02	-2.25	.129	-0.05	0.02	-2.42	.191
17: Parahippocampal	0.02	0.03	0.85	.629	-0.02	0.02	-0.83	.537	-0.04	0.03	-1.39	.296
18: Medial occipital cortex	0.03	0.03	1.26	.470	-0.05	0.02	-2.32	.129	-0.03	0.02	-1.14	.328

Cortical Thickness NMF Network	Fear				Overall Psychopathology				
	B	SE	t	p_{fdr}	B	SE	t	p_{fdr}	R^2*
1: Cingulate cortex	-0.05	0.02	-2.22	.040	-0.03	0.02	-1.54	.249	0.35
2: Medial temporal cortex	-0.07	0.02	-2.85	.009	-0.03	0.02	-1.06	.399	0.17
3: Temporal pole	-0.06	0.02	-2.86	.009	-0.02	0.02	-1.09	.399	0.37
4: Frontal cortex	-0.03	0.02	-1.49	.153	0.05	0.02	2.21	.123	0.38
5: Posterior cingulate cortex	-0.08	0.02	-3.69	.001	-0.04	0.02	-1.90	.149	0.34
6: Superior parietal cortex	-0.03	0.02	-1.30	.204	0.01	0.02	0.38	.748	0.38
7: Superior temporal cortex	-0.05	0.02	-2.14	.045	0.00	0.02	0.00	.997	0.17
8: Dorsomedial prefrontal cortex	-0.01	0.02	-0.43	.665	0.04	0.02	1.74	.186	0.35
9: Insular cortex	-0.05	0.02	-2.23	.040	-0.03	0.02	-1.48	.249	0.29
10: Fusiform cortex	-0.09	0.03	-3.41	.002	-0.06	0.03	-2.28	.123	0.10
11: Inferior temporal cortex	-0.08	0.02	-3.47	.002	-0.01	0.02	-0.50	.694	0.25
12: Right lateral occipital cortex	-0.07	0.02	-3.08	.005	-0.03	0.02	-1.10	.399	0.22
13: Subgenual cingulate, anterior cingulate, and anterior insula	-0.08	0.02	-3.42	.002	-0.06	0.02	-2.71	.061	0.25
14: Inferior prefrontal cortex	-0.05	0.02	-2.39	.031	0.04	0.02	2.03	.128	0.38
15: Intraparietal	-0.04	0.02	-1.70	.107	-0.02	0.02	-0.89	.483	0.33
16: Posterior cingulate (a) and TPJ (b)	-0.09	0.02	-4.38	<.001	-0.09	0.02	-4.25	<.001	0.37
17: Parahippocampal	-0.05	0.03	-2.03	.055	-0.05	0.03	-2.08	.128	0.11
18: Medial occipital cortex	-0.09	0.02	-3.75	.001	-0.02	0.02	-0.69	.589	0.23

* R^2 values are for the full-model.

TABLE S2. Structural covariance networks of volume in relation to anxious-misery, psychosis, behavioral, fear, and overall pathology (n=1394, df=1385)

Volume	Anxious-misery				Psychosis				Behavioral			
NMF Network	B	SE	t	p_{fdr}	B	SE	t	p_{fdr}	B	SE	t	p_{fdr}
1: Cingulate cortex	0.06	0.02	2.23	.029	-0.03	0.02	-1.16	.277	-0.06	0.02	-2.56	.053
2: Medial temporal cortex	0.09	0.02	3.96	<.001	-0.05	0.02	-2.13	.185	-0.05	0.02	-1.99	.072
3: Temporal pole	0.10	0.02	4.28	<.001	-0.02	0.02	-1.12	.277	-0.06	0.02	-2.38	.054
4: Frontal cortex	0.06	0.02	2.31	.025	-0.03	0.02	-1.34	.253	-0.05	0.02	-2.14	.064
5: Posterior cingulate cortex	0.08	0.02	3.35	.002	-0.04	0.02	-1.63	.207	-0.05	0.02	-2.06	.072
6: Superior parietal cortex	0.07	0.03	2.75	.008	-0.04	0.02	-1.92	.185	-0.08	0.02	-3.25	.011
7: Superior temporal cortex	0.04	0.02	1.69	.092	-0.01	0.02	-0.62	.533	-0.02	0.02	-0.65	.516
8: Dorsomedial prefrontal cortex	0.07	0.02	3.02	.005	-0.03	0.02	-1.41	.253	-0.03	0.02	-1.47	.160
9: Insular cortex	0.08	0.03	3.10	.004	-0.03	0.02	-1.41	.253	-0.05	0.02	-2.22	.060
10: Fusiform cortex	0.09	0.02	3.86	<.001	-0.05	0.02	-2.05	.185	-0.08	0.02	-3.28	.011
11: Inferior temporal cortex	0.10	0.02	4.37	<.001	-0.05	0.02	-2.15	.185	-0.03	0.02	-1.44	.160
12: Right lateral occipital cortex	0.08	0.02	3.20	.003	-0.04	0.02	-1.75	.185	-0.04	0.02	-1.56	.144
13: Subgenual cingulate, anterior cingulate, and anterior insula	0.05	0.02	2.06	.042	-0.03	0.02	-1.28	.258	-0.06	0.02	-2.37	.054
14: Inferior prefrontal cortex	0.07	0.02	2.77	.008	-0.04	0.02	-1.74	.185	-0.05	0.02	-1.94	.072
15: Intraparietal	0.06	0.02	2.63	.011	-0.03	0.02	-1.18	.277	-0.05	0.02	-1.95	.072
16: Posterior cingulate (a) and TPJ (b)	0.10	0.02	4.12	<.001	-0.04	0.02	-1.77	.185	-0.04	0.02	-1.83	.088
17: Parahippocampal	0.07	0.02	2.80	.008	-0.04	0.02	-1.74	.185	-0.05	0.02	-2.30	.056
18: Medial occipital cortex	0.09	0.02	3.52	.001	-0.03	0.02	-1.33	.253	-0.06	0.02	-2.52	.053

Volume	Fear				Overall Psychopathology				
NMF Network	B	SE	t	p_{fdr}	B	SE	t	p_{fdr}	R^{2}*
1: Cingulate cortex	-0.05	0.02	-2.11	.061	-0.09	0.02	-3.62	<.001	0.25
2: Medial temporal cortex	-0.07	0.02	-3.19	.008	-0.11	0.02	-4.91	<.001	0.31
3: Temporal pole	-0.07	0.02	-2.80	.015	-0.10	0.02	-4.47	<.001	0.27
4: Frontal cortex	-0.04	0.02	-1.92	.071	-0.11	0.02	-4.93	<.001	0.28
5: Posterior cingulate cortex	-0.04	0.02	-1.77	.092	-0.11	0.02	-4.69	<.001	0.25
6: Superior parietal cortex	-0.02	0.02	-0.84	.423	-0.12	0.02	-4.87	<.001	0.24
7: Superior temporal cortex	-0.01	0.02	-0.57	.567	-0.07	0.02	-3.15	.002	0.26
8: Dorsomedial prefrontal cortex	-0.06	0.02	-2.61	.023	-0.10	0.02	-4.19	<.001	0.30
9: Insular cortex	-0.05	0.02	-1.92	.071	-0.10	0.02	-4.27	<.001	0.22
10: Fusiform cortex	-0.06	0.02	-2.51	.027	-0.12	0.02	-5.13	<.001	0.28
11: Inferior temporal cortex	-0.08	0.02	-3.51	.004	-0.11	0.02	-4.73	<.001	0.33
12: Right lateral occipital cortex	-0.07	0.02	-3.15	.008	-0.11	0.02	-4.76	<.001	0.32
13: Subgenual cingulate, anterior cingulate, and anterior insula	-0.02	0.02	-0.97	.372	-0.10	0.02	-4.19	<.001	0.28
14: Inferior prefrontal cortex	-0.05	0.02	-2.07	.061	-0.10	0.02	-4.31	<.001	0.28
15: Intraparietal	-0.05	0.02	-2.22	.054	-0.09	0.02	-3.85	<.001	0.27
16: Posterior cingulate (a) and TPJ (b)	-0.09	0.02	-3.64	.004	-0.11	0.02	-4.71	<.001	0.26
17: Parahippocampal	-0.05	0.02	-2.05	.061	-0.10	0.02	-4.11	<.001	0.26
18: Medial occipital cortex	-0.07	0.02	-3.00	.010	-0.08	0.02	-3.58	<.001	0.24

* R^{2} values are for the full-model.

TABLE S3. Sensitivity analysis that includes maternal level of education as an additional covariate and excludes 11% of the sample on psychiatric psychotropic medications (n=1226, df=1215)

NMF Network	CT and Fear						Volume and Overall					Volume and Anxious-misery					
	B	SE	t	p	p_{fdr}	R^2*	B	SE	t	p	p_{fdr}	B	SE	t	p	p_{fdr}	R^2*
1: Cingulate cortex	-0.05	0.02	-2.14	.033	.056	0.36	-0.07	0.03	-2.79	.005	.007	0.03	0.03	1.15	.250	.300	0.28
2: Medial temporal cortex	-0.06	0.03	-2.19	.029	.056	0.18	-0.08	0.02	-3.42	.001	.001	0.07	0.03	2.59	.010	.035	0.34
3: Temporal pole	-0.05	0.02	-2.12	.034	.056	0.38	-0.09	0.03	-3.43	.001	.001	0.07	0.03	2.83	.005	.028	0.30
4: Frontal cortex	-0.04	0.02	-1.77	.077	.098	0.38	-0.10	0.02	-4.08	<.001	<.001	0.02	0.03	0.85	.395	.418	0.29
5: Posterior cingulate cortex	-0.10	0.02	-3.97	<.001	.001	0.36	-0.09	0.03	-3.60	<.001	.001	0.05	0.03	1.78	.075	.138	0.29
6: Superior parietal cortex	-0.04	0.02	-1.93	.054	.075	0.40	-0.09	0.03	-3.60	<.001	.001	0.05	0.03	1.77	.076	.138	0.27
7: Superior temporal cortex	-0.04	0.03	-1.59	.112	.125	0.17	-0.06	0.02	-2.52	.012	.013	0.00	0.03	0.16	.872	.872	0.28
8: Dorsomedial prefrontal cortex	-0.02	0.02	-0.82	.411	.411	0.35	-0.08	0.02	-3.13	.002	.002	0.05	0.03	1.83	.068	.138	0.32
9: Insular cortex	-0.02	0.02	-1.00	.318	.337	0.30	-0.09	0.03	-3.31	.001	.002	0.07	0.03	2.42	.016	.047	0.25
10: Fusiform cortex	-0.08	0.03	-3.00	.003	.008	0.11	-0.10	0.02	-4.20	<.001	<.001	0.08	0.03	2.90	.004	.028	0.31
11: Inferior temporal cortex	-0.08	0.03	-3.00	.003	.008	0.26	-0.08	0.02	-3.44	.001	.001	0.07	0.03	2.74	.006	.028	0.37
12: Right lateral occipital cortex	-0.08	0.03	-3.09	.002	.008	0.24	-0.08	0.02	-3.49	.001	.001	0.05	0.03	1.77	.077	.138	0.36
13: Subgenual cingulate, anterior cingulate, and anterior insula	-0.06	0.03	-2.38	.017	.045	0.25	-0.08	0.02	-3.21	.001	.002	0.03	0.03	1.28	.199	.256	0.31
14: Inferior prefrontal cortex	-0.05	0.02	-2.15	.032	.056	0.38	-0.09	0.03	-3.55	<.001	.001	0.04	0.03	1.42	.157	.217	0.30
15: Intraparietal	-0.04	0.02	-1.66	.097	.117	0.34	-0.06	0.02	-2.27	.024	.024	0.02	0.03	0.87	.384	.418	0.30
16: Precuneus (a) and TPJ (b)	-0.08	0.02	-3.46	.001	.003	0.40	-0.09	0.03	-3.52	<.001	.001	0.08	0.03	2.86	.004	.028	0.31
17: Parahippocampal	-0.06	0.03	-2.06	.040	.060	0.12	-0.07	0.03	-2.78	.005	.007	0.04	0.03	1.46	.146	.217	0.29
18: Medial occipital cortex	-0.09	0.03	-3.54	<.001	.003	0.24	-0.06	0.03	-2.49	.013	.014	0.04	0.03	1.64	.102	.167	0.26

* R^2 values are for the full-model.

TABLE S4. Structural covariance networks of cortical thickness and volume in relation to traditional diagnostic categories

Diagnostic Category	N	Average CT				Total Gray Matter Volume			
		B	*SE*	*t*	*p*	*B*	*SE*	*t*	*p*
ADHD	230	-1.83	0.80	-2.43	.015	-15.50	4.66	-3.33	<.001
Agoraphobia	81	-3.54	1.17	-3.03	.003	-24.20	7.01	-3.45	<.001
Conduct disorder	121	-3.44	0.94	-3.67	<.001	-34.22	5.86	-5.85	<.001
Generalized anxiety disorder	27	0.59	1.81	0.33	.744	-1.40	11.03	-0.13	.899
Major depressive disorder	193	-1.84	0.83	-2.22	.027	-18.49	5.10	-3.63	<.001
Obsessive-compulsive disorder	43	-4.05	1.49	-2.71	.007	-27.35	8.82	-3.10	.002
Oppositional defiant disorder	458	-2.20	0.63	-3.52	<.001	-22.10	3.89	-5.69	<.001
Psychosis	399	-2.10	0.66	-3.19	.001	-22.88	3.95	-5.79	<.001
Posttraumatic stress disorder	172	-2.65	0.85	-3.11	.002	-26.57	5.30	-5.02	<.001
Separation anxiety disorder	63	-1.30	1.22	-1.07	.287	-9.72	7.47	-1.30	.194
Social anxiety disorder	328	-2.61	0.70	-3.74	<.001	-18.99	4.09	-4.65	<.001
Specific phobia	426	-0.83	0.65	-1.28	.200	-11.24	3.84	-2.93	.003

**FIGURE S1. Schematic representing network derivation using non-negative matrix factorization**
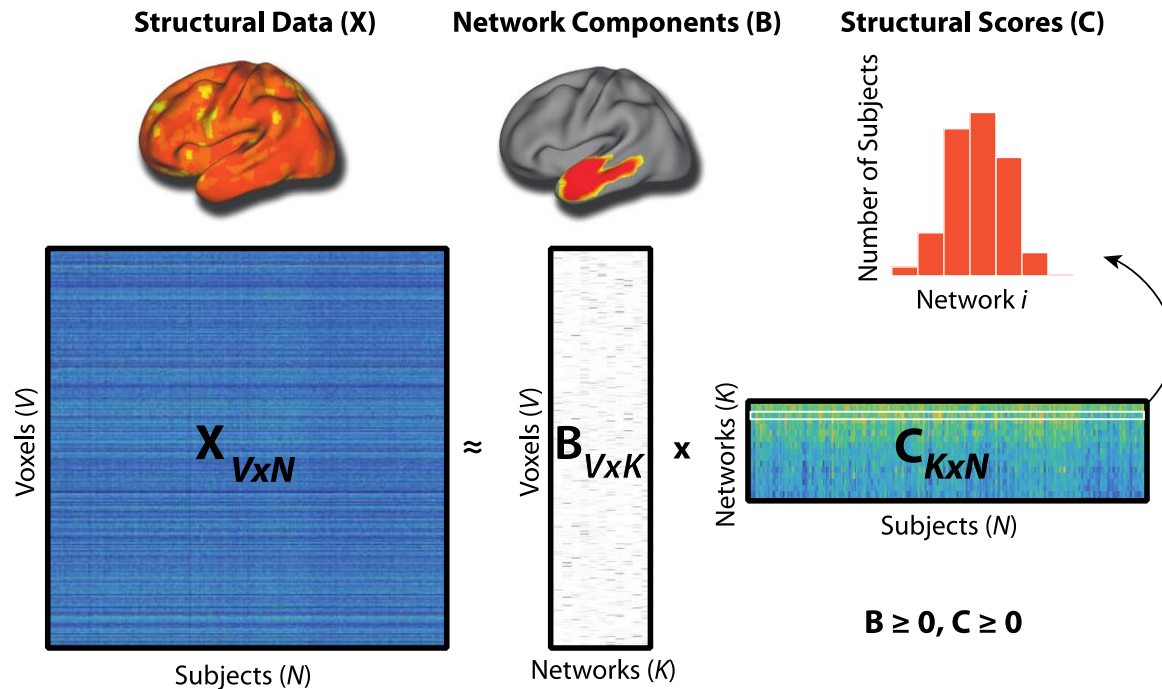
In this schematic, X represents the original data matrix as the product of two matrices, B and C. X contains the whole-brain structural data for each voxel (rows) and for all subjects (columns). Above the X matrix is an example of the whole-brain cortical thickness data for one subject. B is a matrix which contains the reduced number of K networks derived from NMF, and the loadings for each voxel on each of these networks. Above B is one example of NMF network loadings. C is a matrix that contains the subject-specific coefficients for cortical thickness in each network. The histogram above shows a sample row of the C matrix with scores for all subjects in one network. Importantly, both B and C are greater than or equal to 0, thus elements of the factorization are non-negative. Matrices are shown with following dimensions: V = number of voxels, N = number of participants; K = number of networks.

**FIGURE S2. Gradient of reconstruction error for multiple NMF solutions**
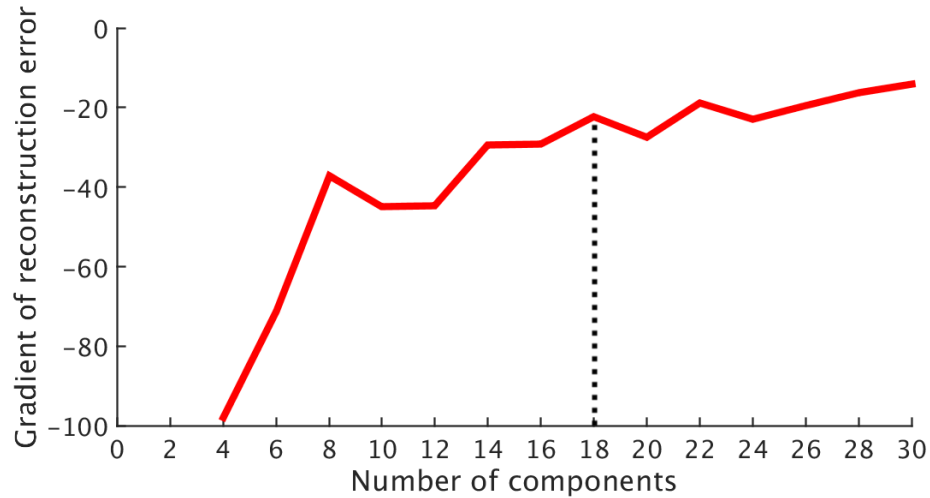
Reconstruction error is plotted for multiple NMF resolutions; the gradient is the difference in reconstruction error as the NMF solution increases by 2 networks. As expected, reconstruction error plateaued as the number of networks increased. The differences in reconstruction error for the solutions between 14 and 30 networks were fairly similar and the final chosen solution of 18 networks is shown with a dotted line. The 18-network solution is consistent with prior work (32). Further, a split-half reliability analysis was also conducted and showed an Adjusted Rand Index of .93, suggesting the 18-network solution is highly reproducible.

FIGURE S3. NMF results are consistent with ROIs derived from JLF
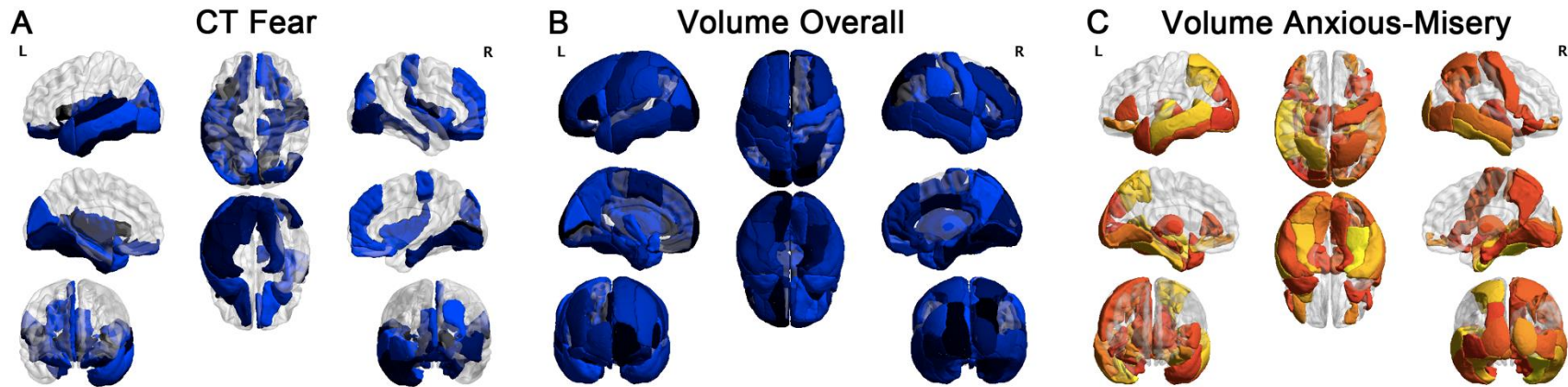
As a sensitivity analysis, structural ROIs were derived from the top performing regional parcellation using a multi-atlas labeling system with joint label fusion (JLF) as implemented in ANTs. The results show highly similar significant regions compared to non-negative matrix factorization (NMF) for **A)** cortical thickness and fear, **B)** volume and overall psychopathology, and **C)** volume and anxious-misery.

FIGURE S4. Structural networks are associated with symptoms above and beyond age, sex, and cognition
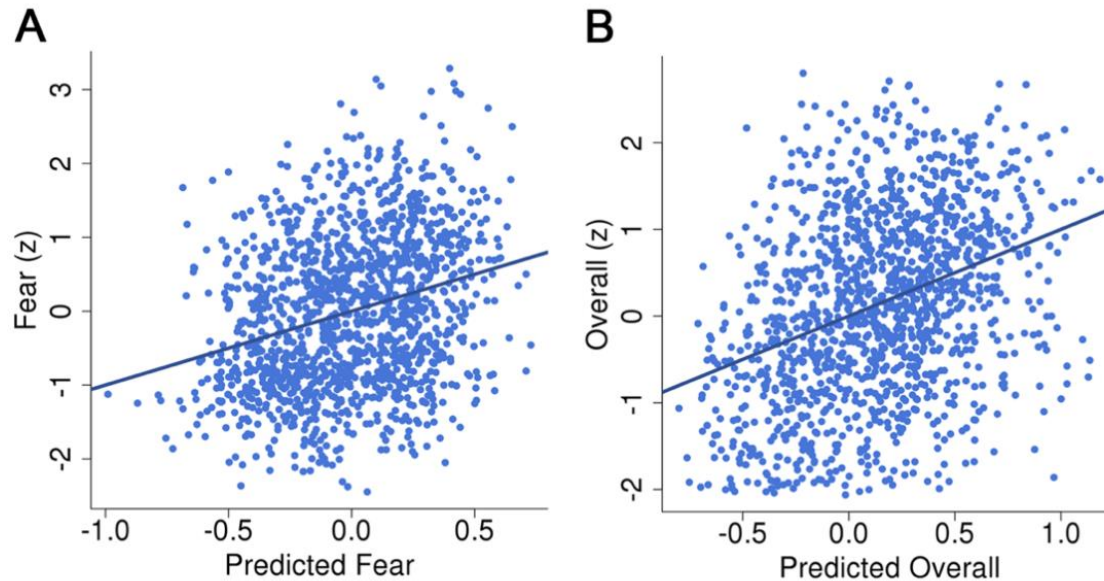
We tested whether structure (cortical thickness or volume) provided information about psychopathology symptoms (fear, overall psychopathology, or anxious-misery) above and beyond demographics (age, sex) and cognitive factors. We compared a null model with only age, sex, and the three cognitive factors of 1) executive function and complex reasoning, 2) social cognition, and 3) episodic memory to a full model with age, sex, the three cognitive factors, and the 18 structural networks. **A)** For cortical thickness, we found that the proportion of variance in fear explained by the predictors improved in the full model compared to the null model. The correlation between the actual fear scores and the predicted fear scores in the full model was .28. **B)** For volume, the proportion of variance in overall psychopathology explained by the predictors also improved in the full model compared to the null model, and showed a correlation of .35 between the actual and predicted overall psychopathology scores.